

Freeze-out and thermalization in relativistic heavy ion collisions

Sourendu Gupta,¹ Debasish Mallick,² Dipak Kumar Mishra,³,
Bedangadas Mohanty,^{2,*} Nu Xu^{4,5}

¹Department of Theoretical Physics, Tata Institute of Fundamental Research,
Homi Bhabha Road, Mumbai 400005, India

²School of Physical Sciences, National Institute of Science Education and Research, HBNI,
Jatni 752050, India

³Nuclear Physics Division, Bhabha Atomic Research Centre, Mumbai 400085, India,

⁴Institute of Modern Physics, Chinese Academy of Sciences,
509 Nanchang Road, Lanzhou 730000, China

⁵College of Physical Science and Technology, Central China Normal University,
152 Luyu Road, Wuhan 430079, China

January 22, 2022

Abstract

High energy heavy-ion collisions in laboratory produce a form of matter that can test Quantum Chromodynamics (QCD), the theory of strong interactions, at high temperatures. One of the exciting possibilities is the existence of thermodynamically distinct states of QCD, particularly a phase of de-confined quarks and gluons. An important step in establishing this new state of QCD is to demonstrate that the system has attained thermal equilibrium. We present a test of thermal equilibrium by checking that the mean hadron yields produced in the small impact parameter collisions as well as grand canonical fluctuations of conserved quantities give consistent temperature and baryon chemical potential for the last scattering surface. This consistency for moments up to third order of the net-baryon number, charge, and strangeness is a key step in the proof that the QCD matter produced

*Chinese Academy of Sciences President's International Fellowship Initiative visiting scientist at Institute of Modern Physics, Lanzhou 730000, China

in heavy-ion collision attains thermal equilibrium. It is a clear indication for the first time, using fluctuation observables, that a femto-scale system attains thermalization. The study also indicates that the relaxation time scales for the system are comparable to or smaller than the life time of the fireball.

Relativistic collisions of heavy-ion are being carried out at the Relativistic Heavy Ion Collider (RHIC) in BNL and the Large Hadron Collider (LHC) facilities in CERN. These experiments have demonstrated the existence of a deconfined state of quarks and gluons, which are the fundamental constituents of baryonic matter. The experiments observe the collective flow of a fireball made of such deconfined matter [1, 2, 3, 4, 5] (see also a review [6]). This state of matter replicates baryonic matter in the universe when it was a few microseconds old. It is also conjectured that the cores of astrophysical objects like neutron stars may contain a related form of baryonic matter, albeit at lower temperature but higher density [7].

By studying the flow of matter in the femto-scale fireballs produced at RHIC and LHC, it has been shown that the ratio of shear viscosity to entropy density, η/s , is the lowest among all known fluids [8, 9]. The values of this ratio extracted from experiment are close to the bounds expected for a strongly coupled quantum fluid [10]. Further, it has been recently shown this fluid has large vortical effect [11].

Theoretical studies of strongly interacting matter using lattice field theory shows a cross over from hadronic matter to a deconfined state of quarks and gluons [12]. Consistent with these expectations, no sign of a phase transition has been found at the top energies in the experiments at RHIC and LHC.

Lattice studies have revealed an experimentally reachable critical point [13, 14, 15] in an extremely rich phase diagram of strongly interacting matter [16, 17, 18, 19]. Currently experimental studies are underway to vary the collision energy in order to study this phase diagram [20, 21, 22]. Experimental data reveals tantalising hints of critical behaviour

[23, 24, 25], but these interpretations of experiments have the underlying assumption that the fireball produced in the collisions should have come to local thermal equilibrium during its evolution. Experimental tests of thermalization are non-trivial for these femto-scale system: not just because the systems are small, but also because they are expanding [20]. This is what we examine critically in this paper.

Systems which are significantly larger than the measuring instruments allow ensembles of measurements on a single system, and one may exploit the hierarchy of scales between the size of the full system, the measuring apparatus, and the microscopic length scales. This allows us to create ensembles of measurements on identical systems by measuring the system at multiple points. This philosophy is used routinely to measure fluctuations in the early universe [26, 27]. On the other hand it is problematic when the measurement involves the whole system. This happens for low-multipole fluctuations in the universe, and is called the cosmic variance problem. For the femto-scale system which we study, the hierarchy of length scales collapses for all measurements, and one constructs the ensemble by repeating the experiment. This requires additional checks to make sure that the repeated trials are indeed comparable.

Another dimension of the problem is whether the system evolves with time or not. Again when the time scale of evolution, of measurement, and the microscopic dynamics are well separated, simplicities emerge. In a static large system, repeated measurements can be made at effectively the same time. This can probe thermodynamic stability such as the convexity of free energies, or the lack of entropy production. However, in quasi-statically evolving systems the entropy may change simply because the temperature changes with time, and not because the system is driven towards or out of equilibrium. When there is no clear hierarchy between the rate of evolution and microscopic relaxation time, then one has to qualify the notion of thermal equilibrium.

Distribution functions are driven out of equilibrium, and different parts may evolve at different rates. For a small decrement of temperature, ΔT , the equilibration of mean energies will require small changes. In a Boltzmann gas, for example, the average energy changes by the factor $3\Delta T/2$. This change is easily made by small exchanges of momentum among those particles which lie near the peak of the thermal distribution, and can proceed quickly. The tail of the distribution, on the other hand, has to change by a large factor. There are two ways for this to happen. One is that particles carrying these rare large momenta collide with others having equally large momenta and both emerge with smaller momentum in one scattering. Another way is for the large momentum particle to collide many times with particles of much smaller momenta and decrease the momentum in small steps. Either route gives longer relaxation times. Similarly, local changes in the chemical potential, $\Delta\mu$, distort the local number distribution, different part of which relax at different rates. Due to such differential relaxation of different parts of the distribution function different moments of the distributions may not correspond to the same temperature and chemical potential. One also knows that approach to a critical point brings with it correlated fluctuations of the whole system in both space and time, thereby increasing relaxation times dramatically. Studying the moments of the number distributions to find evidences for both equilibrium and large departures scenarios are therefore crucial tests for the physics of these femto-systems.

In the relativistic femto-systems created by heavy-ion collisions, the conserved quantities are the net-baryon number (B), strangeness (S) and electric charge (Q). Since these are additive quantum numbers, every anti-particle has a charge opposite to that of the particle, and the net quantum number is the algebraic sum over particles and anti-particles. Conserved quantities measured for the whole system will always be equal to that in the initial state. However, using the limited acceptance of the detector, only a

part of the thermalized system is accessed experimentally and hence can be treated within the framework of grand canonical ensemble. This allows us to measure fluctuations of the conserved quantities.

If the fireballs were static and in thermal equilibrium, they could be described by a temperature, T , and three chemical potentials μ_B , μ_S and μ_Q . Since the system is not static, these four quantities are functions of space and time. One can only observe particles which come to the detector after the last scattering. This region of last scattering is characterized by a specific value of T and chemical potentials which are generally called freezeout parameters. It is common to quote as the freezeout parameters the values of these thermodynamic variables which give the best match between particle yields (i.e means of number distributions) in a statistical model of an ideal gas of hadrons and resonances (HRG)[28, 29, 30, 31, 32]. Characterizing the yield at fixed $\sqrt{s_{NN}}$ and acceptance window by a single set of freezeout parameters was seen to work well for charged hadrons [28, 29]. Characterizing strange and non-strange hadrons by different freezeout conditions works slightly better in some cases [33]. Other variants of the HRG have also been shown to work [34, 35, 36, 37, 38, 39]. However, these HRG models also seem to describe yield data in e^+e^- and pp collisions, where one does not expect thermalized matter to be formed [40, 41, 42]. Similarly, they can describe yields in highly peripheral collisions. These observations introduce a severe uncertainty in the interpretation of the freezeout parameters derived using yields in terms of thermal conditions. Here we propose that a way out of this impasse is to ask for common thermal descriptions of more than just the mean particle number.

Model: The hadron resonance gas (HRG) model that we utilize in this work is briefly discussed below and details can be found at Ref.[31]. In a grand canonical ensemble with a gas of hadrons and resonances, the thermodynamic pressure (P) can be obtained from

the logarithm of partition function in the limit of large volume as

$$P(T, \mu_B, \mu_Q, \mu_S, V) = \frac{T}{V} \sum_i \ln Z_i = \sum_i \pm \frac{T g_i}{2\pi^2} \int d^3k \ln \{1 \pm \exp [(\mu_i - E)/T]\}. \quad (1)$$

where k is the momentum, g_i is the degeneracy factor of the i^{th} species of hadron or resonance, and the plus signs are for Fermions whereas the minus signs are for Bosons. The sum is carried out over all particles in thermal equilibrium with masses up to 2.5 GeV which are listed in Particle Data Group (PDG) booklet.

The freezeout conditions for the fireball are characterized by the temperature T , freezeout volume V , and the three chemical potentials μ_B , μ_Q , and μ_S . If the system is in chemical equilibrium then the chemical potential for the i^{th} species is given by $\mu_i = B_i \mu_B + Q_i \mu_Q + S_i \mu_S$, where B_i , Q_i and S_i are the baryon number, electric charge and strangeness of the particle. In the analysis that we present in this paper, the detector's acceptance and resonance decay effects are taken into account, for details see Ref.[31].

The effect of radial flow (collective expansion of the system) seen in heavy-ion collisions do not affect the moments as they are obtained integrated over the measured p_T range. HRG model calculations with and without flow shows a small difference for the observable studied [31] and those are used as systematic uncertainties associated with the model calculations in the paper.

The grand canonical approach is justifiable as experimental data used in the current work analyses a portion of the fireball produced in heavy-ion collisions. It is akin to an open system, unlike for the data for full 4π coverage which would have required a canonical treatment with exact conservation of charges. In addition, the criteria for applicability of grand canonical ensemble, $VT^3 > 1$ holds true for the bulk of the produced particles in heavy-ion collisions. Such an approach has been widely used to understand the yields

of produced hadrons [20, 43, 44] and fluctuations [45, 46, 47] in the field of high-energy nuclear collisions. Further, as discussed in Ref. [48], the effect of global conservation of charges depends on the fraction of charges accepted in the detector, which is found to be small and within the experimental uncertainties for the data up to third order moment used in the current work.

Observable: In this paper, we study the cumulants of different order such as: $C_1^X = \langle X \rangle$, $C_2^X = \langle (X - \langle X \rangle)^2 \rangle$, $C_3^X = \langle (X - \langle X \rangle)^3 \rangle$, $C_4^X = \langle (X - \langle X \rangle)^4 \rangle - 3(C_2^X)^2$ and so on, where X can be one of B , Q and S . Since the observed cumulants in thermal equilibrium are related to the susceptibilities:

$$C_n^X = (V/T) T^n \chi_X^{(n)}(T, \mu_B), \quad (2)$$

there is a possible way to check thermalization and the predictions of lattice QCD [46, 49, 45, 50, 51, 52]. The n^{th} order generalised susceptibilities ($\chi_X^{(n)}$), where X represents baryon, strangeness or electric charge indices, can be expressed as [13],

$$\chi_X^{(n)}(T, \mu_B, \mu_Q, \mu_S) = \frac{d^n P(T, \mu_B, \mu_Q, \mu_S)}{d\mu_X^n}. \quad (3)$$

Usually ratios of cumulant or products of moments are calculated in order to cancel the dependence on system volume. Experiments use the notation $M = C_1$ for the mean, $\sigma^2 = C_2$ for the variance, $S = C_3/C_2^{3/2}$ for the skewness, and $\kappa = C_4/C_2^2$ for the kurtosis. In terms of these variables, the ratios of cumulants are $\sigma^2/M = C_2/C_1$, $S\sigma = C_3/C_2$ and $\kappa\sigma^2 = C_4/C_2$ [23, 53, 54]. Though all the three ratios of higher cumulants (σ^2/M , $S\sigma$, $\kappa\sigma^2$) and second order off-diagonal cumulants (σ_{XY}^2) [55] reported by the STAR experiment are expected to carry the fluctuation signals, only observables up to third order moments (M , σ_{XY}^2 , σ_{XX}^2 , $S\sigma$) are used in this work. The observable, $\kappa\sigma^2$, will be used elsewhere to test departures from thermal equilibrium. The observables calculated in the HRG model are the same as measured in the experiment.

Experimental Data: The STAR experiment has published measurements on cumulants up to 4th order and their ratios for the net-proton number (NP) [23], the net-kaon number (NK) [53] and the net-charge (NQ) [54]. The experiment has also published second order off-diagonal cumulants [55]. The effect of choosing NP as a proxy of net-baryon and NK as a proxy of net-strangeness has been studied in detail in [56, 57]. Event-by-event net-charge distributions are obtained using the Time Projection Chamber (TPC) and Time of Flight (TOF) detectors at STAR in the momentum range $0.2 < p_T(\text{GeV}/c) < 2.0$ and a pseudo-rapidity range of $|\eta| < 0.5$ [54]. Net-proton distribution is measured [23] using TPC detector only in a momentum range of $0.4 < p_T(\text{GeV}/c) < 0.8$ and net-kaon [53] using both TPC and TOF detector within a momentum range of $0.2 < p_T(\text{GeV}/c) < 1.6$. The second order off-diagonal cumulants σ_{Qp}^2 , σ_{QK}^2 and σ_{pK}^2 representing correlations between electric charge-baryon number, electric charge-strangeness number and baryon-strangeness number are obtained by STAR by detecting particles within of acceptance of $|\eta| < 0.5$ and $0.4 < p_T(\text{GeV}/c) < 1.6$ [55]. All the above measurements are done for small impact parameter (called central 0-5%) Au on Au collisions at a range $\sqrt{s_{NN}} = 7.7\text{--}200$ GeV. The cumulants of distributions are corrected for detector inefficiencies and other analysis artefacts as discussed in [23, 53, 54]. So the experimental data available for this work are the observables, M_{π^+} , M_{π^-} , M_{K^+} , M_{K^-} , M_p , $M_{\bar{p}}$, $\sigma^2(NP)$, $\sigma^2(NK)$, $\sigma^2(NQ)$, σ_{Qp}^2 , σ_{QK}^2 and σ_{pK}^2 , $S\sigma(NP)$, $S\sigma(NK)$ and $S\sigma(NQ)$. It has been previously shown by several authors [58, 59, 61] that the σ^2/M for net-charge and net-protons are not properly explained by several variants of HRG models. The reason has been understood to be due to the acceptance limitation in the measurements — resonance decays can throw part of the charge outside the detector acceptance, thereby increasing the value of σ^2/M over the intrinsic thermal distribution for the fireball. Interestingly the decay distortion is absent from the observables $\sigma^2/M(NK)$ and all three $S\sigma$. In order to deal with the

stochasticity due to decays, we introduce the three volume independent observable using the second order cumulants for the current study: $\sigma_{QK}^2/\sigma^2(NK)$, $\sigma_{pK}^2/\sigma^2(NK)$, and $\sigma_{Qp}^2/\sigma^2(NP)$ [60].

Methodology: The freezeout parameters, namely the T , μ_B , μ_S and μ_Q , are extracted at each $\sqrt{s_{NN}}$, from the experimental data by minimizing

$$\chi^2 = \sum_{i=1}^N \left(\frac{\Delta_i}{E_i} \right)^2 \quad \text{where} \quad \Delta_i = R_i^{\text{exp}} - R_i^{\text{HRG}}, \quad (4)$$

where N is the number of observables used in this calculation. R_i^{exp} and R_i^{HRG} are experimental measurements and HRG model calculations respectively for the i^{th} observable, and E_i is the statistical uncertainty in the experiment.

As a first step in the analysis we tested whether a fit can distinguish between a thermal and a non-thermal system. This was done by taking simulated data obtained from the non-thermal model called UrQMD [62], and trying to extract freezeout conditions from it by the process outlined in Eq. 4. Approximately one million UrQMD events were analyzed for 0-5% Au+Au collisions at each collision energy. In this case we found that the value of $\chi^2/\text{ndf} \sim O(1000 - 10000)$ for all observable rules out a reasonable fit, and the best possible freezeout parameters obtained from the yields, $\sigma^2/M(NP, NK, NQ)$, and $S\sigma(NP, NK, NQ)$ are quite different. Even carrying out the studies without σ^2/M for net-charge and net-protons in UrQMD yields a $\chi^2/\text{ndf} \sim O(100 - 10000)$. Since UrQMD model is known to reproduce many other aspects of the final state obtained in heavy-ion collisions like multiplicity and mean p_T [63], this shows that accidental agreement of the data with the HRG model is unlikely. We have additionally repeated the analysis using a different non-thermal model that includes parton degrees of freedom, A Multi Phase Transport (AMPT) model [64], for Au+Au collisions at $\sqrt{s_{NN}} = 200$ GeV and found that the thermal fit failed.

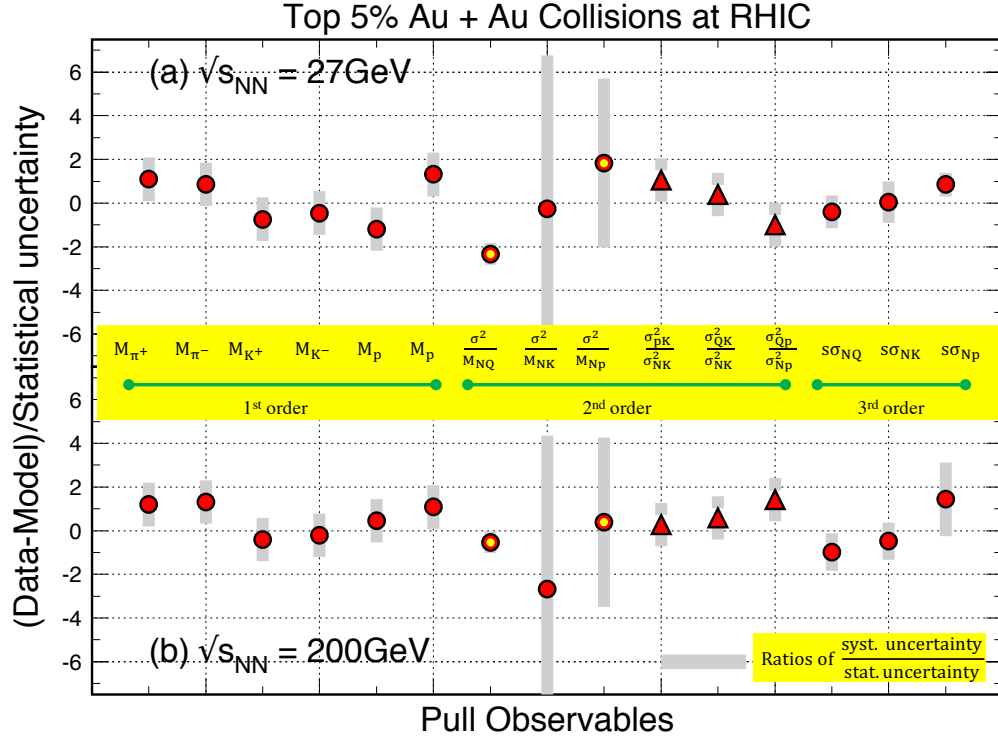


Figure 1: Detailed comparison of the best fit predictions of the HRG model at (a) $\sqrt{s_{NN}} = 27\text{ GeV}$ and (b) $\sqrt{s_{NN}} = 200\text{ GeV}$, which minimizes χ^2 given in Eq. (4) with the experimental measurements. This representative case at two collision energies shows the difference between data and HRG model (Δ) divided by the statistical uncertainty along the ordinate for each of the observables mentioned in the abscissa. The $\sigma^2/M(\text{NQ})$ and $\sigma^2/M(\text{NP})$ values shown as open circles are scaled down by a factor 100. The figure also shows a comparison of the magnitudes of systematic and statistical uncertainties, since the former are not included in the definition of χ^2 to improve the discriminatory power of the fits.

Results: In Figure 1 we show the quality of a fit to fifteen pieces of data (shown in x-axis) at $\sqrt{s_{NN}} = 27$ GeV and $\sqrt{s_{NN}} = 200$ GeV obtained by varying only T , μ_B , μ_S and μ_Q . The σ^2/M for net-charge and net-protons behaves quite differently from the others due to the effect of resonance decay as discussed above. However, the ratios of second order cumulants ($\sigma_{QK}^2/\sigma^2(NK)$, $\sigma_{pK}^2/\sigma^2(NK)$, and $\sigma_{Qp}^2/\sigma^2(NP)$) are well explained by the model.

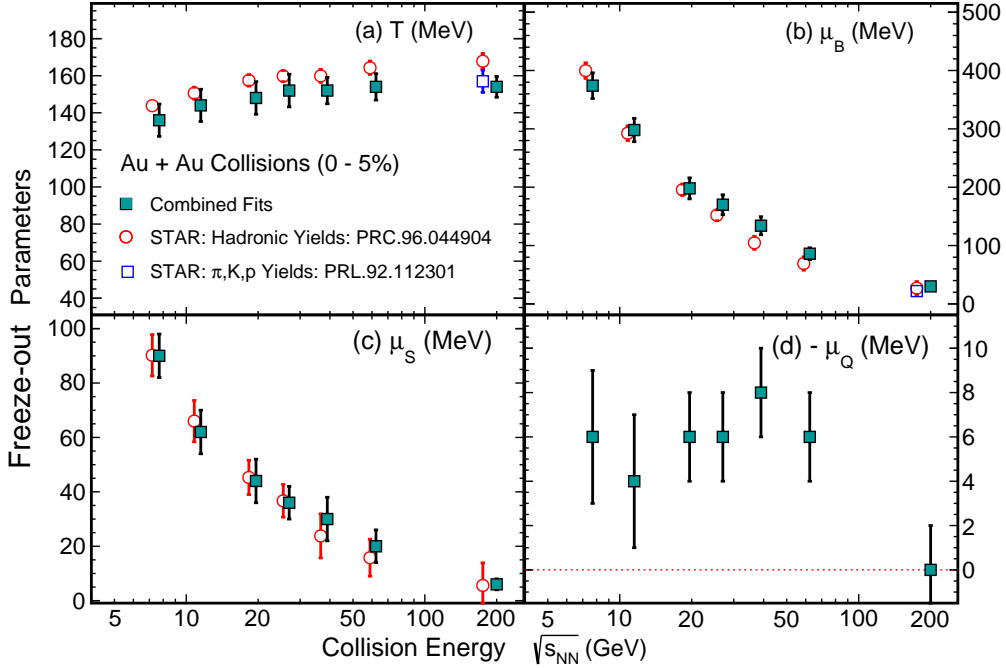


Figure 2: The best fit parameters of the HRG model at different $\sqrt{s_{NN}}$ obtained by fitting data for central Au+Au collisions. Shown as red open circles (with points slightly displaced for clarity of presentation) are the comparison of the freezeout parameters to those obtained using only the mean yields of various produced hadrons by STAR experiment [20]. Also shown as open blue squares are the comparison of the freeze-out parameters at $\sqrt{s_{NN}} = 200$ GeV obtained by fitting to the mean yields of only π^\pm , K^\pm and $p(\bar{p})$.

At every $\sqrt{s_{NN}}$, we fitted the parameters of the HRG model to the thirteen observables (M_{π^+} , M_{π^-} , M_{K^+} , M_{K^-} , M_p , $M_{\bar{p}}$, $\sigma^2/M(NK)$, $\sigma_{QK}^2/\sigma^2(NK)$, $\sigma_{pK}^2/\sigma^2(NK)$, $\sigma_{Qp}^2/\sigma^2(NP)$, $S\sigma(NP)$, $S\sigma(NK)$ and $S\sigma(NQ)$) shown in Figure 1 as solid circles. In Fig. 2 we show

the best fit values of T , μ_B , μ_S and μ_Q as a function of $\sqrt{s_{NN}}$. The χ^2/ndf are of the $O(1)$, except for $\sqrt{s_{NN}} = 7.7$ GeV, where the value is 11.9. The results of the fits, which now include higher second and third order moments of particle multiplicity distributions are in good agreement with those obtained only using the mean yields of produced particles (shown as red open circles) by STAR experiment [20]. The slight difference in T values arises because of inclusion of multi-strange hadrons in the fits to the yields. As shown in the figure, for $\sqrt{s_{NN}} = 200$ GeV (as blue open square), using similar observables as in the current study, i.e the yields of π^\pm , K^\pm and $p(\bar{p})$, has a better agreement with our results. Including systematic uncertainties in the experimental data by adding in quadrature improves the χ^2/ndf values to 1.0 and 4.6 for $\sqrt{s_{NN}} = 200$ and 7.7 GeV, respectively. We have verified that the measured p_T distributions of pion, kaon, proton and the anti-particles for 0-5% Au+Au collisions at $\sqrt{s_{NN}} = 200$ and 19.6 GeV are reproduced using a thermal model with the extracted thermal parameters and average radial flow velocity of $0.55c$ and $0.46c$, respectively.

In Figure 3 we show the ΔT and $\Delta\mu_B$, the differences between the best fit value of T and μ_B obtained from yields of π^\pm , K^\pm and $p(\bar{p})$, second order cumulants $\sigma^2/M(NK)$, $\sigma_{QK}^2/\sigma^2(NK)$, $\sigma_{pK}^2/\sigma^2(NK)$, $\sigma_{Qp}^2/\sigma^2(NP)$ and those obtained by fitting the three $S\sigma(NP)$, $S\sigma(NK)$ and $S\sigma(NQ)$ for various $\sqrt{s_{NN}}$. Results for both central (left panel) and peripheral (right panel) collisions are shown. Since the minimum number of observables in a set is three, we have kept T and μ_B parameters of HRG model free, fixed μ_S values to those from STAR experiment [20] and μ_Q values to zero, for this test only. We note that in central collisions for $\sqrt{s_{NN}} = 19.6$ GeV and higher collision energies, the best fit freezeout parameters obtained from different observables agree with each other within uncertainties. We further note that in peripheral collisions the different observables give very different freezeout conditions. A similar study with UrQMD central Au+Au collision

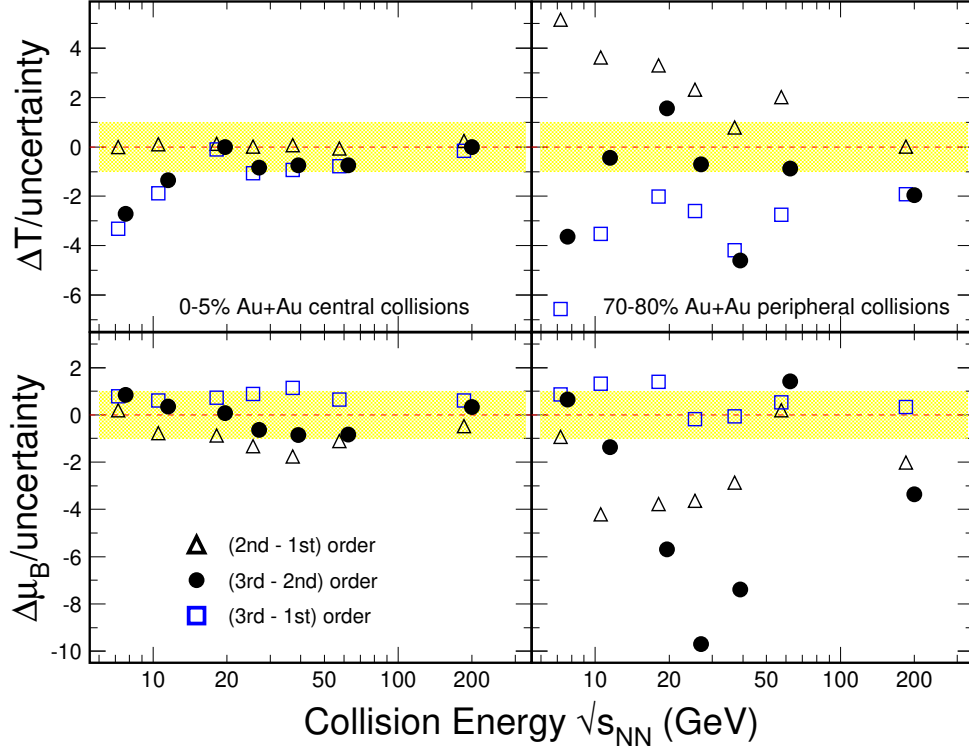


Figure 3: Detailed comparison of the best fit parameters of the HRG model at different $\sqrt{s_{NN}}$ obtained by fitting to different subsets of the data. The difference in temperature (ΔT) and baryon chemical potential ($\Delta\mu_B$) from the third order to second order, third order to first order and second order to the first order moments are shown as filled-circles, open-squares and open-triangles, respectively. The figures show that consistent values of the freezeout parameters are obtained from different subsets of the data in central collisions at all $\sqrt{s_{NN}}$ except, possibly, the two smallest values. In peripheral collisions fits to different subsets of data give significantly different results, implying that thermalization is not seen.

data yields ΔT and $\Delta\mu_B$ values normalized to the respective uncertainties that varies in the range -12 to 18 , indicating no agreement between HRG thermal parameter values from the UrQMD data. The fact that results from HRG model are in excellent agreement with experimental data on various orders of fluctuation measure and with similar values of extracted thermal parameters T and μ_B within the uncertainties, demonstrates that the

QCD matter produced in central Au on Au collisions at RHIC has attained thermalization at least for $\sqrt{s_{NN}} = 19.6$ GeV and above.

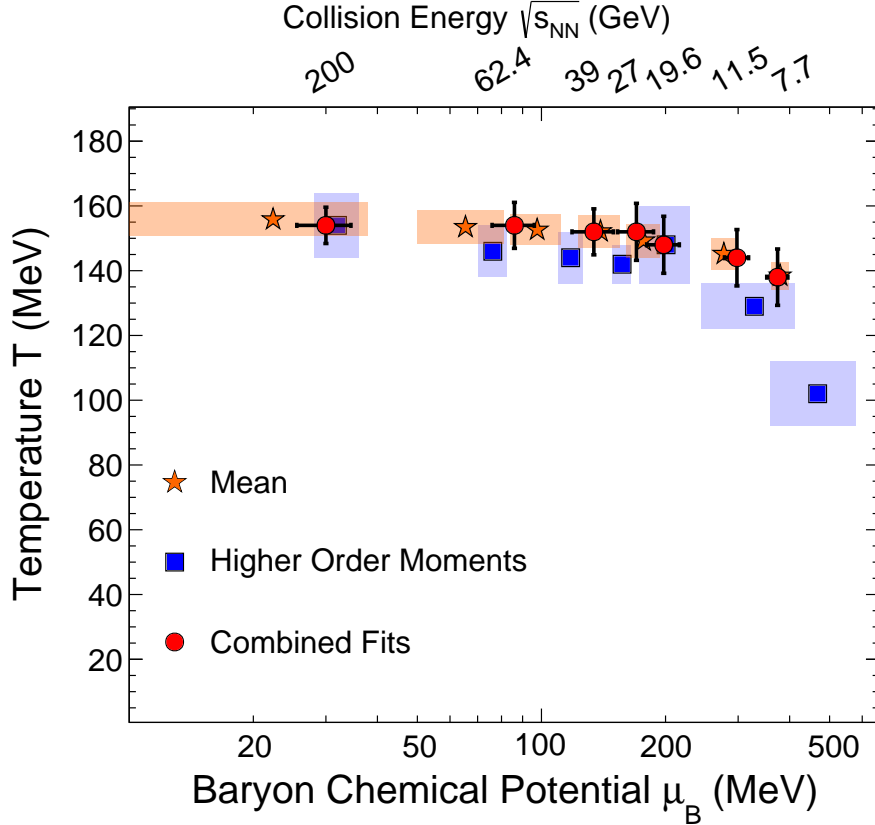


Figure 4: T and μ_B values at freeze-out for Au on Au collision (0–5% centrality) at $\sqrt{s_{NN}} = 7.7$ –200 GeV. The circles represent the best fit T and μ_B values (black lines the uncertainties) obtained from the comparison of experimental yields of pion, kaon and proton, σ^2/M of net-kaon, $\sigma_{QK}/\sigma^2(NK)$, $\sigma_{pK}/\sigma^2(NK)$, $\sigma_{Qp}/\sigma^2(NP)$ and $S\sigma$ of net-proton, net-kaon and net-charge to corresponding results from HRG model with all four parameters free. Square markers represent T and μ_B values (blue band the uncertainties) obtained from the simultaneous comparison of 2nd-order and 3rd-order moments to corresponding results from the HRG model. The stars are the results corresponding to the mean values of the yields of pion, kaon and protons. Coloured bands show uncertainties on freeze-out T and μ_B values.

Our final results are shown in Figure 4. This shows the results of the extraction of the freezeout parameters simultaneously using the 13 observables discussed earlier at each

$\sqrt{s_{NN}}$ GeV. Also shown are the freeze-out T and μ_B extracted from data and the HRG model using the combination of M_π , M_K and M_p , and combined higher order moments of σ^2/M of net-kaon, $\sigma_{QK}^2/\sigma^2(NK)$, $\sigma_{pK}^2/\sigma^2(NK)$, $\sigma_{Qp}^2/\sigma^2(NP)$, $S\sigma(NP, NK, NQ)$ observable for Au on Au collisions at $\sqrt{s_{NN}} = 7.7\text{--}200$ GeV. The uncertainties are systematic associated with the implementation of various assumptions in the model and statistical, both added in quadrature. The model assumptions varied includes, radial flow effect, interactions through excluded volume effect, fixing some of the model parameters like μ_Q and μ_S from other measurements, resonance decay and considering width of resonances. The extracted T and μ_B values are in agreement among all the three observables at each $\sqrt{s_{NN}}$ within the uncertainties upto $\sqrt{s_{NN}} = 19.6$ GeV, below that there are clear indications of deviations. The agreement between freezeout parameters extracted from different pieces of data shows that at freezeout the system is thermalized at large $\sqrt{s_{NN}}$.

Conclusions:

We have reported a study of thermalization at the last stages of the evolution of the fireball created in heavy-ion collisions. The analysis of yields of hadrons (*i.e.*, the means of the hadron number distributions) is known to be explained in thermal models for central and peripheral collisions of nuclei, in pp and e^+e^- collisions, and for synthetic data produced through event generators like UrQMD. This raises doubts about whether the analysis of yields is sufficient to tell us about thermalization of the fireball.

We found that a sensitive test of thermalization is the simultaneous description of yields as well as the event-to-event fluctuation measures σ^2/M (for net-kaons), σ^2/M , $\sigma_{QK}^2/\sigma^2(NK)$, $\sigma_{pK}^2/\sigma^2(NK)$, $\sigma_{Qp}^2/\sigma^2(NP)$ and $S\sigma$ (for net-charge, net-protons and net-kaons). The variance measure σ^2/M for net-charge and net-protons has been found to be sensitive to acceptance, due to resonance decays. As a result, we cannot use these measures along with the rest. Instead we use the observables, $\sigma_{QK}^2/\sigma^2(NK)$, $\sigma_{pK}^2/\sigma^2(NK)$,

$\sigma_{Qp}^2/\sigma^2(NP)$. Agreement of all these observables for central Au+Au collisions with thermal gas predictions under common freezeout conditions is a strong indication that not only the region near the peak of the distribution, but also some part of the tail begins to approach a thermal distribution. This indicates that for the central Au+Au collisions at large $\sqrt{s_{NN}}$ the medium densities are high enough, resulting in sufficient interactions among the constituents, to lead to thermalization. The relaxation time scales for the system are comparable to or smaller than the life time of the fireball.

Our studies shows a clear indication that an expanding femto-scale QCD system formed in central collisions of high energy heavy-ions [20] attains thermalization. Furthermore, this test shows that neither synthetic data, nor peripheral collisions can be considered as thermal or behaves like a bulk matter in thermodynamics. Interestingly the test also indicates that central collisions at the two lowest $\sqrt{s_{NN}}$ may not be thermal. This lack of thermalization can be due to the fireballs being too dilute to ever come to equilibrium, or for there to be long relaxation time at these energies. Further studies are needed to establish which is the case, and thereby explore the part of the phase boundary which may be probed by the low-energy experiments.

For a thermal distribution, all orders of the cumulants should correspond to the same set of thermal parameters. We have not included fourth and higher order cumulants in this study. The higher order cumulants are, in principle, more sensitive to correlation lengths, and therefore are more sensitive probes of physics related to critical point and the nature of phase transition.

Data availability. The data that support the findings of this study are available from the corresponding author upon reasonable request.

Code availability. The hadron resonance model code is available from the corresponding author upon reasonable request.

Acknowledgements We thank Dr. Subhasis Samanta and Mr. Ashish Pandav for discussions related to this work.

References

- [1] Adams, J. *et al.*, Experimental and theoretical challenges in the search for the quark gluon plasma: The STAR Collaboration's critical assessment of the evidence from RHIC collisions, *Nucl. Phys.* **A757**, 102 (2005).
- [2] Adcox, K. *et al.*, Formation of dense partonic matter in relativistic nucleus-nucleus collisions at RHIC: Experimental evaluation by the PHENIX collaboration, *Nucl. Phys.* **A757**, 184 (2005).
- [3] Aamodt, K. *et al.*, Elliptic flow of charged particles in Pb-Pb collisions at 2.76 TeV, *Phys. Rev. Lett.* **105**, 252302 (2010).
- [4] Aamodt, K. *et al.*, Suppression of Charged Particle Production at Large Transverse Momentum in Central Pb-Pb Collisions at $\sqrt{s_{NN}} = 2.76$ TeV, *Phys. Lett.* **B696**, 30 (2011).
- [5] Chatrchyan, S. *et al.*, Observation and studies of jet quenching in PbPb collisions at nucleon-nucleon center-of-mass energy = 2.76 TeV, *Phys. Rev.* **C84**, 024906 (2011).
- [6] Gyulassy, M. and McLerran, L.D., New forms of QCD matter discovered at RHIC, *Nucl. Phys.* **A750**, 30 (2005).
- [7] Lattimer, J.M. and Prakash, M., The physics of neutron stars, *Science* **304**, 536 (2004).

- [8] Csernai, L.P., Kapusta, J.I. and McLerran, L.D., On the Strongly-Interacting Low-Viscosity Matter Created in Relativistic Nuclear Collisions, *Phys. Rev. Lett.* **97**, 152303 (2006).
- [9] Romatschke, P. and Romatschke, U., Viscosity Information from Relativistic Nuclear Collisions: How Perfect is the Fluid Observed at RHIC?, *Phys. Rev. Lett.* **99**, 172301 (2007).
- [10] Kovtun, P., Son, D.T. and Starinets, A.O., Viscosity in strongly interacting quantum field theories from black hole physics, *Phys. Rev. Lett.* **94**, 111601 (2005).
- [11] Adamczyk, L. *et al.*, Global Λ hyperon polarization in nuclear collisions: evidence for the most vortical fluid, *Nature* **548**, 62 (2017).
- [12] Aoki, Y., Endrodi, G., Fodor, Z., Katz, S.D. and Szabo, K.K., The Order of the quantum chromodynamics transition predicted by the standard model of particle physics, *Nature* **443**, 675 (2006).
- [13] Gavai, R.V. and Gupta, S., The Critical end point of QCD, *Phys. Rev.* **D71**, 114014 (2005).
- [14] Datta, S., Gavai, R.V. and Gupta, S., Quark number susceptibilities and equation of state at finite chemical potential in staggered QCD with $N_t=8$, *Phys. Rev.* **D95**, 054512 (2017).
- [15] D'Elia, M., High-Temperature QCD: theory overview, *Nucl. Phys.* **A982**, 99 (2019).
- [16] Stephanov, M.A., Rajagopal, K. and Shuryak, E.V., Event-by-event fluctuations in heavy ion collisions and the QCD critical point, *Phys. Rev.* **D60**, 114028 (1999).

- [17] Hatta, Y. and Stephanov, M.A., Proton number fluctuation as a signal of the QCD critical endpoint, *Phys. Rev. Lett.* **91**, 102003 (2003).
- [18] Stephanov, M.A., Non-Gaussian fluctuations near the QCD critical point, *Phys. Rev. Lett.* **102**, 032301 (2009).
- [19] Asakawa, M., Ejiri, S. and Kitazawa, M., Third moments of conserved charges as probes of QCD phase structure, *Phys. Rev. Lett.* **103**, 262301 (2009).
- [20] Adamczyk, L.*et al.*, Bulk Properties of the Medium Produced in Relativistic Heavy-Ion Collisions from the Beam Energy Scan Program, *Phys. Rev.* **C96**, 044904 (2017).
- [21] Braun-Munzinger, P. and Wambach, J., The Phase Diagram of Strongly-Interacting Matter, *Rev. Mod. Phys.* **81**, 1031 (2009).
- [22] Fukushima, K. and Hatsuda, T., The phase diagram of dense QCD, *Rept. Prog. Phys.* **74**, 014001 (2011).
- [23] Adamczyk, L.*et al.*, Energy Dependence of Moments of Net-proton Multiplicity Distributions at RHIC, *Phys. Rev. Lett.* **112**, 032302 (2014).
- [24] Aggarwal, M.M.*et al.*, Higher Moments of Net-proton Multiplicity Distributions at RHIC, *Phys. Rev. Lett.* **110**, 022302 (2010).
- [25] Luo, X., Energy Dependence of Moments of Net-Proton and Net-Charge Multiplicity Distributions at STAR, *PoS CPOD* **2014**, 019 (2015).
- [26] Smoot, G.F.*et al.*, Structure in the COBE differential microwave radiometer first year maps, *Astrophys. J.* **396**, L1 (1992).

- [27] Komatsu, E.*et al.*, Seven-Year Wilkinson Microwave Anisotropy Probe (WMAP) Observations: Cosmological Interpretation, *Astrophys. J. Suppl.* **192**, 18 (2011).
- [28] Cleymans, J., Oeschler, H., Redlich, K. and Wheaton, S., Comparison of chemical freeze-out criteria in heavy-ion collisions, *Phys. Rev.* **C73**, 034905 (2006).
- [29] Andronic, A., Braun-Munzinger, P. and Stachel, J., Hadron production in central nucleus-nucleus collisions at chemical freeze-out, *Nucl. Phys.* **A772**, 167 (2006).
- [30] Becattini, F., Gazdzicki, M., Keranen, A., Manninen, J. and Stock, R., Chemical equilibrium in nucleus nucleus collisions at relativistic energies, *Phys. Rev.* **C69**, 024905 (2004).
- [31] Garg, P., Mishra, D.K., Netrakanti, P.K., Mohanty, B., Mohanty, A.K., Singh, B.K., and Xu, N., Conserved number fluctuations in a hadron resonance gas model, *Phys. Lett.* **B726**, 691 (2013).
- [32] Andronic, A., Braun-Munzinger, P., Redlich, K. and Stachel, J., Decoding the phase structure of QCD via particle production at high energy, *Nature* **561**, 321 (2018).
- [33] Chatterjee, S., Godbole, R.M. and Gupta, S., Strange freezeout, *Phys. Lett.* **B727**, 554 (2013).
- [34] Venugopalan, R. and Prakash, M., Thermal properties of interacting hadrons, *Nucl. Phys.* **A546**, 718 (1992).
- [35] Yen, G.D., Gorenstein, M.I., Greiner, W. and Yang, S.N., Excluded volume hadron gas model for particle number ratios in A+A collisions, *Phys. Rev.* **C56**, 2210 (1997).
- [36] Chatterjee, S., Godbole, R.M. and Gupta, S., Stabilizing hadron resonance gas models, *Phys. Rev.* **C81**, 044907 (2010).

- [37] Vovchenko, V., Gorenstein, M.I. and Stoecker, H., van der Waals Interactions in Hadron Resonance Gas: From Nuclear Matter to Lattice QCD, *Phys. Rev. Lett.* **118**, 182301 (2017).
- [38] Samanta, S. and Mohanty, B., Criticality in a Hadron Resonance Gas model with the van der Waals interaction, *Phys. Rev.* **C97**, 015201 (2018).
- [39] Chatterjee, S., Mishra, D., Mohanty, B. and Samanta, S., Freezeout systematics due to the hadron spectrum, *Phys. Rev.* **C96**, 054907 (2017).
- [40] Becattini, F., A Thermodynamical approach to hadron production in e+ e- collisions, *Z. Phys.* **C69**, 485 (1996).
- [41] Becattini, F. and Heinz, U.W., Thermal hadron production in p p and p anti-p collisions, *Z. Phys.* **C76**, 269 (1997).
- [42] Das, S., Mishra, D., Chatterjee, S. and Mohanty, B., Freeze-out conditions in proton-proton collisions at the highest energies available at the BNL Relativistic Heavy Ion Collider and the CERN Large Hadron Collider, *Phys. Rev.* **C95**, 014912 (2017).
- [43] Braun-Munzinger, P. and Stachel, J., The quest for the quark-gluon plasma, *Nature* **448**, 302 (2007).
- [44] Becattini, F., Bleicher, M., Kollegger, T., Schuster, T., Steinheimer, J. and Stock, R. Hadron Formation in Relativistic Nuclear Collisions and the QCD Phase Diagram, *Phys. Rev. Lett.* **111**, 082302 (2013).
- [45] Gavai, R.V. and Gupta, S., Lattice QCD predictions for shapes of event distributions along the freezeout curve in heavy-ion collisions, *Phys. Lett.* **B696**, 459 (2011).

- [46] Bazavov, A.*et al.*, Freeze-out Conditions in Heavy Ion Collisions from QCD Thermodynamics, *Phys. Rev. Lett.* **109**, 192302 (2012).
- [47] Borsanyi, S., Fodor, Z., Katz, S. D., Krieg, S., Ratti, C. and Szabo, K. K. Freeze-out parameters from electric charge and baryon number fluctuations: is there consistency?, *Phys. Rev. Lett.* **113**, 052301 (2014).
- [48] Bzdak, A., Koch, V., and Skokov, V., Baryon number conservation and the cumulants of the net proton distribution, *Phys. Rev.* **C87**, 014901 (2013).
- [49] Gupta, S., Finding the critical end point of QCD: Lattice and experiment, *PoS CPOD 2009*, 025 (2009).
- [50] Gupta, S., Luo, X., Mohanty, B., Ritter, H.G. and Xu, N., Scale for the Phase Diagram of Quantum Chromodynamics, *Science* **332**, 1525 (2011).
- [51] Cheng, M.*et al.*, Baryon Number, Strangeness and Electric Charge Fluctuations in QCD at High Temperature, *Phys. Rev.* **D79**, 074505 (2009).
- [52] Bellwied, R., Borsanyi, S., Fodor, Z., Katz S.D. and Ratti, C. Is there a flavor hierarchy in the deconfinement transition of QCD?, *Phys. Rev. Lett.* **111**, 202302 (2013).
- [53] Adamczyk, L.*et al.*, Collision Energy Dependence of Moments of Net-Kaon Multiplicity Distributions at RHIC, *Phys. Lett.* **B785**, 551 (2018).
- [54] Adamczyk, L.*et al.*, Beam energy dependence of moments of the net-charge multiplicity distributions in Au+Au collisions at RHIC, *Phys. Rev. Lett.* **113**, 092301 (2014).

- [55] Adamczyk, L.*et al.*, Collision-energy dependence of second-order off-diagonal and diagonal cumulants of net-charge, net-proton, and net-kaon multiplicity distributions in Au + Au collisions, *Phys. Rev.* **C100**, 014902 (2019).
- [56] Kitazawa, M. and Asakawa, M., Relation between baryon number fluctuations and experimentally observed proton number fluctuations in relativistic heavy ion collision, *Phys. Rev.* **C86**, 024904 (2011).
- [57] Zhou, C., Xu, J., Luo, X. and Liu, F., Cumulants of event-by-event net-strangeness distributions in Au+Au collisions at $\sqrt{s_{\text{NN}}}=7.7\text{-}200$ GeV from UrQMD model, *Phys. Rev.* **C96**, 014909 (2017).
- [58] Mishra, D.K, Garg, P., Netrakanti, P.K. and Mohanty, A.K., Effect of resonance decay on conserved number fluctuations in a hadron resonance gas model, *Phys. Rev.* **C94**, 014905 (2016).
- [59] Nahrgang, M., Bluhm, M., Alba, P., Bellwied, R. and Ratti, C., Impact of resonance regeneration and decay on the net-proton fluctuations in a hadron resonance gas, *Eur. Phys.* **C75**, 573 (2015).
- [60] Gavai, R. V. and Gupta, S., Fluctuations, strangeness and quasi-quarks in heavy-ion collisions from lattice QCD, *Phys. Rev.* **D73**, 014004 (2006).
- [61] Alba, P., Alberico, W., Bellwied, R., Bluhm, M., Mantovani Sarti, V., Nahrgang, M. and Ratti, C., Freeze-out conditions from net-proton and net-charge fluctuations at RHIC, *Phys. Lett.* **B738**, 305 (2014).
- [62] Bleicher, M.*et al.*, Relativistic hadron hadron collisions in the ultrarelativistic quantum molecular dynamics model, *J. Phys.* **G25**, 1859 (1999).

- [63] Petersen, H., Bleicher, M., Bass, S. A. and Stocker, H., UrQMD v2.3: Changes and Comparisons, *arXiv:0805.0567* (2008).
- [64] Lin, Z. W., Ko, C. M., Li, B. A., Zhang, B. and Pal, S., A Multi-phase transport model for relativistic heavy ion collisions, *Phys. Rev.* **C72**, 064901 (2005).